# Nanoparticles activate the NLR pyrin domain containing 3 (Nlrp3) inflammasome and cause pulmonary inflammation through release of IL-1α and IL-1β

Amir S. Yazdi[a], Greta Guarda[a], Nicolas Riteau[b], Stefan K. Drexler[a], Aubry Tardivel[a], Isabelle Couillin[b], and Jürg Tschopp[a,1]

[a]Department of Biochemistry, University of Lausanne, CH-1066 Epalinges, Switzerland; and [b]Laboratory of Molecular Immunology and Embryology, University of Orleans and Centre National de la Recherche Scientifique, F-45071 Orleans, France

Edited by Marc Feldmann, Imperial College London, London, United Kingdom, and approved October 1, 2010 (received for review June 13, 2010)

**Nanoparticles are increasingly used in various fields, including biomedicine and electronics. One application utilizes the opacifying effect of nano-$TiO_2$, which is frequently used as pigment in cosmetics. Although $TiO_2$ is believed to be biologically inert, an emerging literature reports increased incidence of respiratory diseases in people exposed to $TiO_2$. Here, we show that nano-$TiO_2$ and nano-$SiO_2$, but not nano-ZnO, activate the NLR pyrin domain containing 3 (Nlrp3) inflammasome, leading to IL-1β release and in addition, induce the regulated release of IL-1α. Unlike other particulate Nlrp3 agonists, nano-$TiO_2$–dependent-Nlrp3 activity does not require cytoskeleton-dependent phagocytosis and induces IL-1α/β secretion in nonphagocytic keratinocytes. Inhalation of nano-$TiO_2$ provokes lung inflammation which is strongly suppressed in IL-1R– and IL-1α–deficient mice. Thus, the inflammation caused by nano-$TiO_2$ in vivo is largely caused by the biological effect of IL-1α. The current use of nano-$TiO_2$ may present a health hazard due to its capacity to induce IL-1R signaling, a situation reminiscent of inflammation provoked by asbestos exposure.**

caspase-1 | titanium dioxide | silica dioxide

Nanoparticles are single particles with a diameter less than 100 nm (1). Nanomaterials are increasingly used for manufacturing industrial items, such as antibacterial surface coatings and semiconductors. The most frequently used nanoparticles are inorganic metal oxides such as silica dioxide ($SiO_2$) and titanium dioxide ($TiO_2$), due to their large surface-to-volume ratio (2). In particular, nano-$TiO_2$ is frequently used as white pigment in many everyday products such as white paint, paper, and plastics, and their use is especially prevalent in cosmetics (3).

Although μm-sized and larger $TiO_2$ particles are believed to be biologically inert (4), an augmented frequency of respiratory diseases in workers exposed to $TiO_2$ was reported in the late 1980s (5). Supporting this observation, several recent studies demonstrated that pulmonary uptake of $TiO_2$ nanoparticles worsened respiratory diseases such as pulmonary fibrosis or lipopolysaccharide (LPS)-induced lung inflammation in vivo (6, 7). The particle size of $TiO_2$ was a critical factor in triggering this pulmonary inflammatory response (8, 9).

Cytokines of the interleukin-1 family, such as interleukin-1α (IL-1α), interleukin-1β (IL-1β), and interleukin-18 (IL-18) are potent mediators of innate immunity. They are produced as proforms, which are further processed upon activation. Pathways leading to IL-1α processing, which is active both as pro–IL-1α and as cleaved fragment, are yet to be characterized in detail, but were reported to involve the $Ca^{2+}$-dependent protease calpain (10). Besides its function as an autocrine growth factor, IL-1α is known to drive sterile inflammation, in particular in response to dying cells (11). Compared with IL-1α processing and activation, the mechanisms mediating pro–IL-1β and pro–IL-18 maturation are better characterized. Pro-IL–1β and pro-IL–18 are cleaved by the protease caspase-1, that itself is autoactivated through caspase-1 clustering within large multiprotein complexes called inflammasomes (12). To date four inflammasomes are functionally characterized: the Nlrp1 (NLR pyrin domain containing 1, Nalp1), Nlrp3 (NLR pyrin domain containing 3, Nalp3), Nlrc4 (NLR containing a caspase recruitment domain 4, Ipaf), and AIM2 (absent in melanoma) inflammasomes. The best-characterized inflammasome consists of three main components, the Nod-like receptor (NLR)-family protein, Nlrp3, procaspase-1, and the ASC (apoptosis speck-like protein containing a CARD) adapter, which bridges interactions between the former proteins (12). Following autoactivation via inflammasome assembly, caspase-1 cleaves IL-1β, whose biologically active form is then secreted.

The potent actions of mature IL-1β dictate that its synthesis and secretion are tightly regulated. A first signal, such as Toll-like receptor activation, triggers synthesis of pro–IL-1β by transcriptional induction, whereas a second stimulus leads to inflammasome oligomerization, caspase-1 autoactivation, and caspase-1–dependent cleavage and release of the biologically active, mature IL-1β. This second signal, by which an active inflammasome complex is formed, is triggered by an ever-expanding group of chemically and biologically unrelated danger-associated molecular patterns (DAMPs) or pathogen-associated molecular patterns (PAMPs) (13). Whereas Nlrp3 inflammasome-dependent inflammation promotes pathogen clearance in a number of infection models, such as *Candida albicans* (14) and *Klebsiella pneumonia* (15), the Nlrp3 inflammasome can also initiate pathological inflammatory reactions in response to endogenous or exogenous danger signals such as ATP (16), monosodium urate crystals (MSU) (17), UVB irradiation (18), and the environmental pollutants, silica and asbestos (19, 20). Although data suggest that potassium efflux (13), cathepsin B (19), and/or the generation of reactive oxygen species (ROS) (20) may modulate inflammasome activation, the exact molecular mechanisms mediating inflammasome activation remain elusive (21).

## Results

**Nanoparticles Activate the Nlrp3 Inflammasome in Myeloid Cells and Lead to IL-1β Secretion in Primary Human Keratinocytes.** To determine the possible IL-1–stimulatory effect of metallic nanoparticles, the human macrophage cell line THP1, was stimulated with various nanoparticles for 6 h. In contrast to ZnO (15 nm), both $TiO_2$ (anatase, 20 nm or rutile, 80 nm) and $SiO_2$ (15 nm) induced caspase-1 cleavage and IL-1β secretion (Fig. 1*A*). Because the organ primarily exposed to everyday metallic nanoparticles is the skin, we also stimulated primary human keratinocytes with nanoparticles (Fig. 1*B*).

Author contributions: A.S.Y., I.C., and J.T. designed research; A.S.Y., G.G., N.R., S.K.D., A.T., and I.C. performed research; A.S.Y., G.G., N.R., S.K.D., A.T., and I.C. analyzed data; and A.S.Y. and J.T. wrote the paper.

The authors declare no conflict of interest.

This article is a PNAS Direct Submission.

[1]To whom correspondence should be addressed. E-mail: Jurg.Tschopp@unil.ch.

This article contains supporting information online at www.pnas.org/lookup/suppl/doi:10.1073/pnas.1008155107/-/DCSupplemental.

Similar to macrophages, human keratinocytes secreted mature IL-1β in a dose-dependent manner following exposure to nano-$TiO_2$ and nano-$SiO_2$ but not carbon nanotubes, another nanoparticle, which is used primarily in electronic and material science.

To examine whether mouse and human cells behaved similarly, mouse bone marrow-derived dendritic cells (BMDC) (Fig. 1*C*) and bone marrow-derived macrophages (BMDM) (Fig. S1) were treated with nano-$TiO_2$ and nano-$SiO_2$. Nano-$TiO_2$ and nano-$SiO_2$ were potent stimuli for IL-1β secretion in both murine myeloid cell types, whereas release of inflammasome-independent cytokines such as TNF were minimally affected by nano-$TiO_2$ stimulation as compared with the TLR9 agonist CpG DNA, which induced TNF secretion without activating inflammasome-dependent IL-1β secretion (Fig. S2).

As particulate danger signals (e.g., asbestos, MSU, and alum) trigger secretion of mature IL-1β via the Nlrp3 inflammasome, we hypothesized that the Nlrp3 inflammasome may also mediate responses to nano-$TiO_2$ and nano-$SiO_2$. To test this hypothesis, we treated human and mouse macrophages in which Nlrp3 inflammasome components were knocked down or knocked out, respectively, with nano-$TiO_2$ or nano-$SiO_2$. THP1 cells stably infected with shRNA directed against caspase-1 or Nlrp3 (Fig. 1*A*) or BMDCs from $ASC^{-/-}$ or $Nlrp3^{-/-}$ mice (Fig. 1*C*) did not secrete IL-1β in response to nano-$TiO_2$ or nano-$SiO_2$, indicating that the Nlrp3 inflammasome mediated responses to these agonists. In contrast, knockdown or knockout of the related NLR family member, IPAF (Nlrc4) which can also mediate inflammasome assembly, did not impair IL-1β secretion (Fig. 1*A*, Fig. S1).

**Phagocytosis Is Not Required for Inflammasome Activation by Nano-$TiO_2$.** The precise mechanism of inflammasome activation remains poorly characterized at present; however, potassium efflux and intracellular ROS have been proposed to be criticial for Nlrp3 inflammasome activation in response to "classic" Nlrp3 agonists. To further characterize the activating capacity of nanoparticles in this context, we examined whether Nlrp3 inflammasome activity was suppressed by the ATP-sensitive potassium channel inhibitor, glibenclamide or the chemical ROS scavenger (2R,4R)-4-aminopyrrolidine-2, 4-dicarboxylate (APDC). As for "classic" Nlrp3 agonists such as MSU, cellular pretreatment with glibenclamide or APDC diminished inflammasome-dependent IL-1β secretion triggered by nanoparticles (Fig. S3*A*).

Although the above results suggested the current inflammasome activation scheme proposed for other particles, we found an important difference between nano-$TiO_2$ and known particulate activators such as MSU, alum, hemozoin, and μm-sized $SiO_2$ (20). Whereas these above-mentioned particulates can activate the Nlrp3 inflammasome in myeloid cells, they do not trigger activation in keratinocytes (Fig. 2*A* and *B*). This is likely to reflect the low capacity of keratinocytes to phagocytose particles. In contrast, small diameter (15 nm) but not large diameter (1.5 μm) $SiO_2$ could activate the inflammasome in keratinocytes (Fig. 2*B*), whereas both nano-sized and μm-sized $SiO_2$ activated the Nlrp3 inflammasome in myeloid cells (Fig. 2*A*), suggesting that the inflammasome-activating signal was triggered without the need for particle phagocytosis. In support of this, disruption of actin-mediated phagocytosis by cytochalasin D was unable to suppress nanoparticle-induced IL-1β secretion in macrophages (Fig. 2*C*). Electron microscopy studies further revealed that mainly clustered $TiO_2$ was located free in the cytoplasm of THP1 cells and not located in phagosomes or lysososmes, as would be expected if they were internalized by phagocytosis (Fig. 2*D*). To further elucidate other possible mechanisms of nanoparticle uptake, THP1 cells were either treated with methyl-β-cyclodextrin to disrupt lipid raft-mediated endocytosis

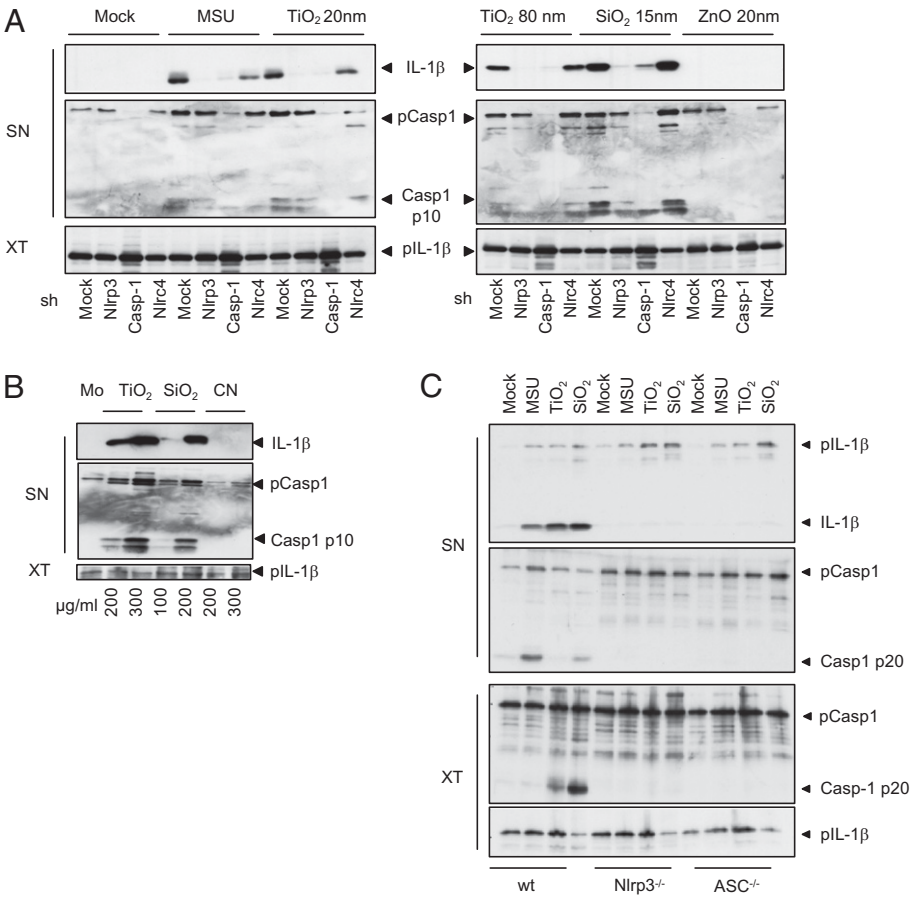


**Fig. 1.** Titanium and silica nanoparticles activate the Nlrp3 inflammasome in murine and human macrophages and human keratinocytes. (*A*) THP1 cells stimulated with MSU (300 μg/mL), $TiO_2$ 20 nm (200 μg/mL), $TiO_2$ 80 nm (200 μg/mL), $SiO_2$ 15 nm (200 μg/mL), and ZnO 15 nm (200 μg/mL) for 6 h and analyzed by Western blot. (*B*) Human primary keratinocytes stimulated with the indicated concentrations of $TiO_2$, 20 nm, $SiO_2$, 15 nm secreted IL-1β and cleaved caspase-1, whereas carbon nanotube exposure did not trigger caspase-1 cleavage. (*C*) Murine macrophages treated with MSU (300 μg/mL), nano-$TiO_2$ (200 μg/mL), or nano-$SiO_2$ (200 μg/mL) released IL-1β in an Nlrp3- and ASC-dependent manner. SN, supernatants; XT, cell extracts. Results are representative of three independent experiments.

filipin or nystatin to block the caveolae-dependent endocytic pathway or chlorpromazine hydrochloride to inhibit clathrin-mediated endocytosis but nano-TiO2–mediated inflammasome activation could not be blocked. (Fig. S3 *B–D*)

**Recruitment of Neutrophils upon I.P. Injection of Nano-$TiO_2$ Is Completely IL-1R–, ASC-, and IL-1α–Dependent.** Taken together, the above results suggested a proinflammatory activity of nano-$TiO_2$ and nano-$SiO_2$ in vitro. We used an established inflammatory peritonitis model (17) to confirm such a role in vivo. In this model, i.p. injection of inflammasome activators drives the influx of neutrophilic granulocytes to the peritoneal cavity. Compared with the solvent control, $TiO_2$ evoked significant neutrophil recruitment 6 h postinjection (Fig. 3*A*). The influx of neutrophils was accompanied by significant sercretion of IL-1β and IL-6 into the peritoneal cavity, while cytokine levels for IL-1α and TNF remained unchanged (Fig. S4*A*). When signaling by both IL-1α and IL-1β was blocked through deficiency in their common receptor, IL-1 receptor (IL-1R), mice exhibited strongly reduced neutrophil influx (Fig. 3*B*). In strict accordance with impaired neutrophil recruitment, a drastic decrease in IL-6 secretion was detected in IL-$1R^{-/-}$ mice, suggesting the dependence of IL-6 secretion on IL-1R signaling (Fig. S4*B*). As the ex vivo findings indicated a critical function for the inflammasome components ASC and Nlrp3 in the response to specific nanoparticles, we also examined $TiO_2$-dependent neutrophil influx in mice deficient in ASC and Nlrp3. Whereas $TiO_2$-induced peritonitis appreciably depended on the ASC adapter, surprisingly, Nlrp3 deficiency did not significantly affect $TiO_2$-induced peritonitis (Fig. 3 *C* and *D*).

Due to our observation that IL-1R deficiency more strongly suppressed $TiO_2$-dependent neutrophil influx compared with ASC or Nlrp3 deficiency, we hypothesized that IL-1α and IL-1β may act in concert to mediate neutrophil influx via their common receptor. Indeed, IL-1α deficiency protected mice from inflammatory cell recruitment (Fig. 3*E*).

**Recruitment of Neutrophils upon I.P. Injection of Nano-$TiO_2$ only Depends on NLRP3 After Depletion of IL-1α.** As the effects of IL-1α appeared to dominate over Nlrp3/IL-1β in this in vivo setting, we reexamined the effect of Nlrp3 deficiency following IL-1α depletion. Following injection of a neutralizing anti-IL–1α antibody, Nlrp3 deficiency significantly suppressed neutrophil influx compared with WT, indicating that both IL-1α and IL-1β can mediate $TiO_2$-induced peritonitis, although the effect of IL-1α predominates (Fig. 3*F*).

**Nano-$TiO_2$ Induces the Release of IL-1α in a Partially Nlrp3- and ASC-Dependent Manner in Myeloid Cells and Keratinocytes in Vitro.** As the peritonitis model suggested a major role for IL-1α in $TiO_2$-dependent inflammation in vivo, we next investigated whether nanoparticles regulated the secretion of IL-1α by murine dendritic cells (DCs) in vitro. Whereas release of IL-1β by MSU or nano-$TiO_2$ was completely dependent on ASC and Nlrp3 as expected (Fig. 3*G*), IL-1α release displayed only a partial dependency on ASC and Nlrp3 (Fig. 3*H*). The partial ASC dependency of IL-1α release was also apparent in murine keratinocytes (Fig. 3*I*).

**Cutaneous Exposure to $TiO_2$ Does Not Lead to a Clinically or Histologically Visible Inflammation.** Data from the peritonitis model and the in vitro data provided proof of principle that $TiO_2$ can induce IL-1–dependent inflammatory responses. However, the two most common routes of nano-$TiO_2$ exposure to humans are via the skin (e.g., application of nano-$TiO_2$–containing cosmetics) and the lungs (e.g., dust inhalation). To more closely mimic a physiological route of cutaneous exposure, we treated shaved back skin of mice with either a single application of $TiO_2$ or PBS dissolved in olive oil or for chronic exposure once daily over a period of 5–10 consecutive days. In agreement with previous reports suggesting that $TiO_2$ nanoparticles do not penetrate into living skin (22, 23), we found that application of the nanoparticle emulsion or its vehicle control did not lead to clinically visible inflammation. Histologically, 8/11 (72%) mice treated with one single application of $TiO_2$ displayed acanthosis (epidermal thickening) without any inflammatory infiltrate, whereas the PBS-treated mice displayed epidermal alterations in 2/11 (18%) cases. Acanthosis without inflammatory infiltrate might be due to mechanical irritation and could be caused by the mice scratching or licking away the $TiO_2$. Upon chronic exposure, the incidence of epidermal

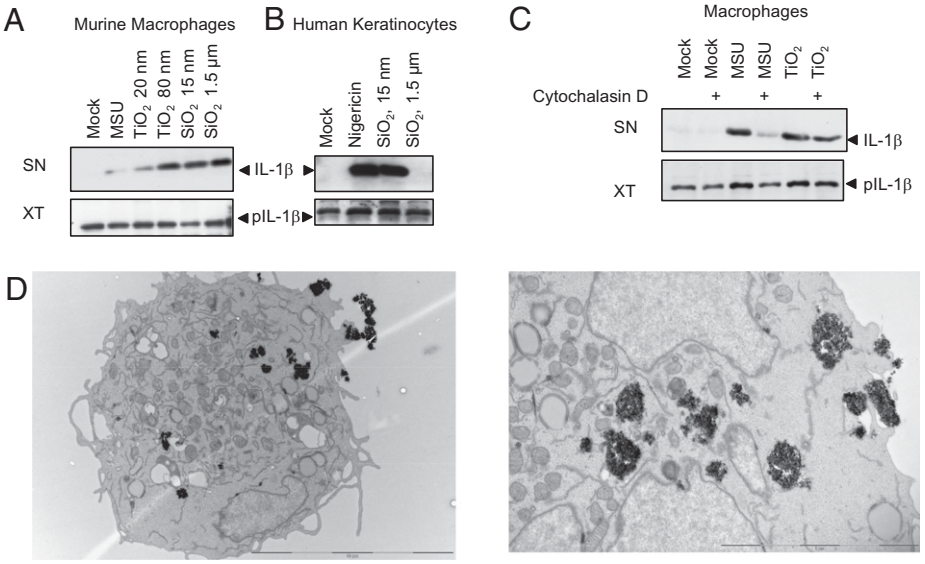


**Fig. 2.** Phagocytosis is not essential for nanoparticle-induced inflammasome activation. (*A*) Bone marrow-derived macrophages released IL-1β upon stimulation with MSU (300 μg/mL), $TiO_2$ 20 nm (200 μg/mL), $TiO_2$ 80 nm (200 μg/mL), $SiO_2$ 15 nm (200 μg/mL), and $SiO_2$ 1.5 μm (200 μg/mL). (*B*) In contrast, human keratinocytes released mature, cleaved IL-1β only upon exposure to nano-$SiO_2$ (200 μg/mL) and not to μm-sized $SiO_2$ (200 μg/mL). (*C*) Actin polymerization blockade by Cytochalasin D (1 μM) impaired MSU-induced inflammasome activation without affecting $TiO_2$-dependent IL-1β secretion. Results are representative of three independent experiments. (*D*) TEM images of THP1 cells stimulated with nano-$TiO_2$. $TiO_2$ aggregates were free in the cytoplasm and not located in phagosomes.

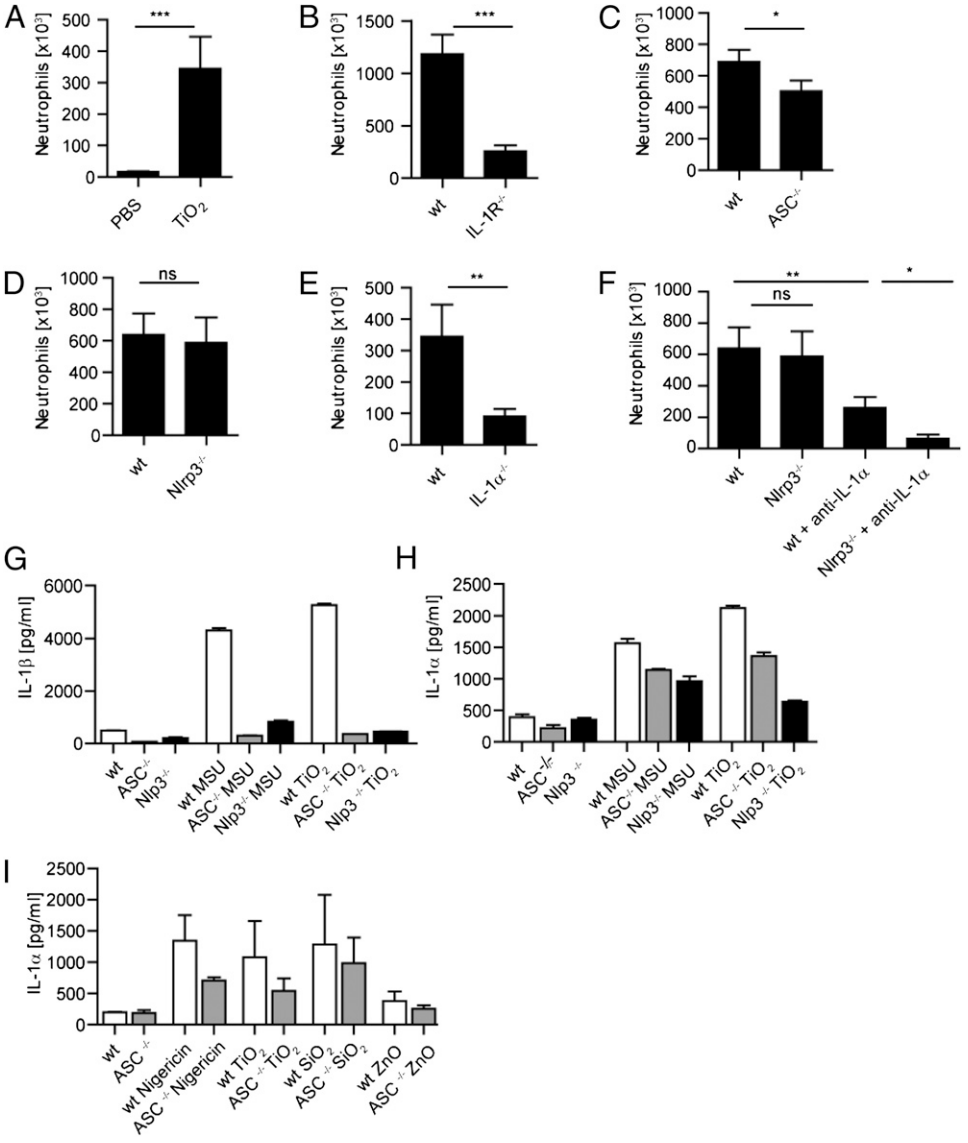


**Fig. 3.** Role of the inflammasome and IL-1α in murine models of $TiO_2$-induced peritonitis and in murine BMDCs and primary murine keratinocytes. (*A*) I.p. injection of nano-$TiO_2$ induced the recruitment of neutrophils to the peritoneal cavity. (*B–F*) The recruitment of inflammatory cells depended upon the presence of (*B*) IL-1R, (*C*) ASC, and (*E*) IL-1α, whereas the inflammatory response was only clearly dependent on Nlrp3 following IL-1α depletion (*D* and *F*). (*$P < 0.05$; **$P < 0.01$; ***$P < 0.001$; NS, nonsignificant, $n$ = 7–10 mice per group). (*G*) Upon stimulation with MSU (300 μg/mL) or nano-$TiO_2$ (200 μg/mL) release of IL-1β was completely abolished in Nlrp3- or ASC-deficient murine BMDCs, whereas the release of (*H*) IL-1α only partially depended on Nlrp3 and ASC. (*I*) Murine keratinocytes secreted IL-1α in a partially ASC-dependent manner upon stimulation with Nigericin (5 μM), nano$TiO_2$ (200 μg/mL), and nano-$SiO_2$ (200 μg/mL), whereas exposure to nano-ZnO (200 μg/mL) did not trigger IL-1α secretion. Results are representative of three independent experiments.

thickening did not further increase and still no inflammatory infiltrates were detectable.

**Pulmonary Inflammation upon Intranasal Exposure of Nano-$TiO_2$ Requires IL-1R, ASC, Caspase-1, and IL-1α.** We next investigated the effect of pulmonary exposure to nano-$TiO_2$. A single dose of intranasally administered $TiO_2$ induced an inflammatory response leading to neutrophil recruitment in the bronchoalveolar lavage fluid (BALF), and IL-1R or caspase-1 deficiency significantly blocked neutrophil influx (Fig. 4*A*). Similar to the observations in the peritonitis model, neutrophil influx depended significantly on the presence of the adapter protein ASC, but exhibited only a partial dependence on Nlrp3, which did not reach significance (Fig. 4 *B* and *C*). As for the peritonitis model, neutrophil recruitment was highly dependent on IL-1α (Fig. 4*C*), and so the effects of IL-1α in this model may mask the potential contribution of IL-1β/Nlrp3. In accordance with our observation in the peritonitis model, only a minor secretion of IL-1α and TNF into the BALF could be observed, whereas $TiO_2$ caused a prominent increase of IL-1β and IL-6 (Fig. 4*D*). Regarding total lung tissue, an induction of both IL-1α and IL-1β could be observed after the administration of $TiO_2$, reflecting an increased synthesis of the two cytokines.

## Discussion

As the use of nanotechnology in our daily consumption products is expanding at a rapid pace, we investigated the inflammatory capacity of one of the most commonly used nanoparticles, $TiO_2$. Previous in vitro and in vivo experiments (24) and postexpositional analysis (5) suggested $TiO_2$ was able to induce inflammation; however, the mechanisms underlying such inflammation were unclear. We present here that, like other environmental irritants such as asbestos or silica, $TiO_2$ and $SiO_2$ nanoparticles are sensed by the Nlrp3 inflammasome (20).

Despite the identification and characterization of numerous sterile or microbial activators of the Nlrp3 inflammasome, the precise mechanism mediating inflammasome activation by these diverse stimuli remains to be determined. Interestingly, nano-$TiO_2$ only partly followed the current scheme for particulate-mediated activation. Like asbestos and silica, nano-$TiO_2$ induces the production of ROS (3) and ROS scavengers block $TiO_2$-dependent IL-1β secretion; nanoparticle-dependent inflammasome activation also appears to depend upon intracellular potassium levels. In contrast to large-diameter, classic particulate Nlrp3 agonists that require phagocytosis, uptake of nanoparticles appeared to occur independently of a functional actin cytoskeleton. Such a mechanistic divergence from the classic particulate activation scheme is

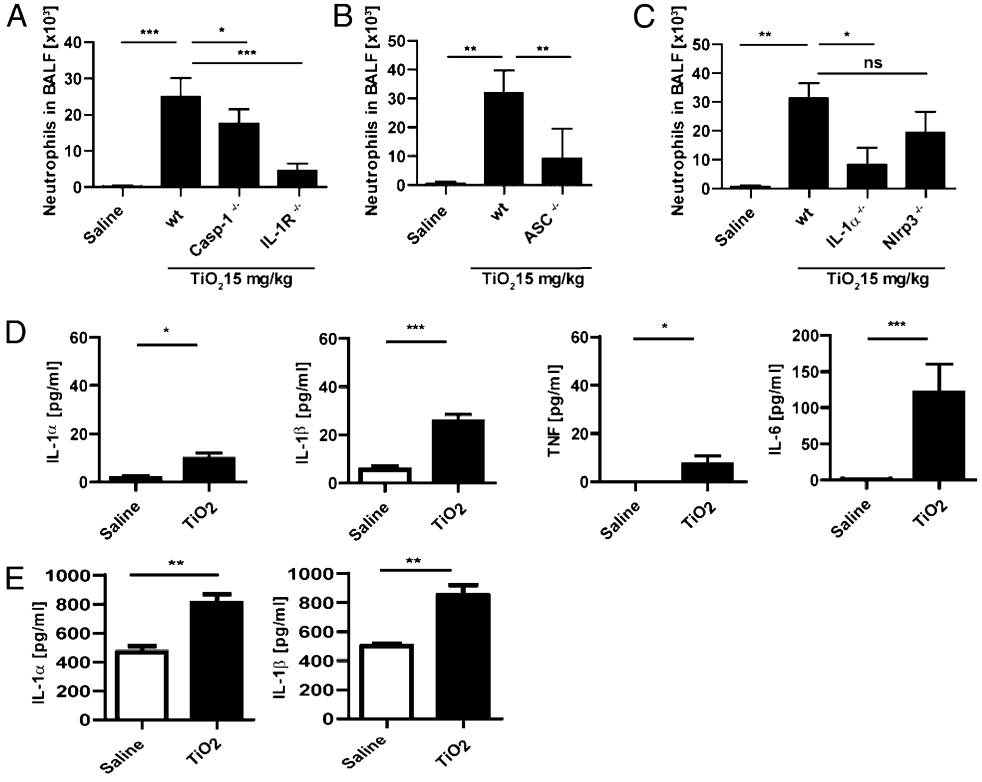


**Fig. 4.** Pulmonary exposure to $TiO_2$. Intranasal application of nano-$TiO_2$ triggered the recruitment of neutrophils to the bronchioalveolar fluid (BALF). Neutrophil recruitment was clearly dependent on (*A*) IL-1R, caspase-1, (*B*) ASC, and (*C*) IL-1α, whereas the recruitment did not significantly depend on Nlrp3. (*D*) Intranasal application of nano-$TiO_2$ induced the secretion of IL-6 and IL-1β into the BALF, whereas TNF- and IL-1α production was only slightly increased. (*E*) In total lung tissue, significantly increased levels of IL-1α and IL-1β could be observed (*$P < 0.05$; **$P < 0.01$; ***$P < 0.001$; NS, nonsignificant; $n = 6$–8 mice per group).

further supported by the ability of nanoparticles to activate primary keratinocytes, which unlike professional phagocytic cells such as macrophages, only ingest small organelles such as melanosomes. However, the exact mechanism of nano-$TiO_2$ uptake remains elusive, as blocking lipid raft-mediated, caveolin-dependent, or clathrin-dependent endocytosis did not efficiently block IL-1β secretion.

In addition to ASC-, Nlrp3-, and caspase-1–dependent secretion of mature IL-1β, we found that nano-$TiO_2$ triggers secretion of another IL-1 family member, IL-1α, in both myeloid and epithelial cells. Interestingly, IL-1α secretion also depends, albeit partly, on the Nlrp3 inflammasome, in accordance with previous results in caspase-1–deficient mice (25).

The in vivo results presented here clearly demonstrate an IL-1R–dependent proinflammatory activity of nano-$TiO_2$ in the lung and peritoneum, which exhibits similar potency to MSU and asbestos, which cause gout and asbestosis, respectively. Moreover, the extreme potency of nano-$TiO_2$ is reflected by its capability to release both IL-1α and IL-1β and is further highlighted by the fact that it can induce the secretion of IL-1 by keratinocytes, a feature not shared with typical particulates. Our results obtained in lung and peritoneal inflammation models indicate the dominance of IL-1α over the biological contribution of IL-1β/Nlrp3.

Our data suggest that nano-$TiO_2$ should be used with greater caution than is currently used. The manufacture of $TiO_2$ nanoparticles is a huge industry; about 2 million tons per year are produced worldwide. In addition to paint, cosmetics, sunscreen, and vitamins, nanoparticles can be found in toothpaste, food colorants, nutritional supplements, and hundreds of other personal care products. When this widespread usage is considered in light of the data presented above, the potential risk of inflammation-driven cancer is a particular concern, especially for people occupationally exposed to high concentrations of $TiO_2$ nanoparticles. Better precautions must be taken to limit the ingestion of these particles, both in manufacturing and in everyday contact with nanoparticle-containing substances.

Similar words of caution were expressed in the last century following the first evidence for association between lung inflammation and asbestos inhalation. Yet it took almost 100 y, and countless fatalities, until asbestos was banned from use. Given that asbestos and $TiO_2$ exert similar proinflammatory activities via IL-1R signaling through the activation of either IL-1α and IL-1β, we hope that future decisions will be made to prevent possible morbidity and perhaps mortality.

## Materials and Methods

**Mice.** C57BL/6J, Nlrp3$^{-/-}$ (17), Asc$^{-/-}$, Ipaf$^{-/-}$ (26), IL-1 α (27), IL-1R$^{-/-}$, and caspase-1$^{-/-}$ (25) mice (on C57BL/6J background) and BALB/c and IL-1R$^{-/-}$ (28) mice (on BALB/c background) were housed at the animal facility at the University of Lausanne or the Transgenose Institute (Centre National de la Recherche Scientifique, Orleans, France). All animal experiments followed the French government's ethical and animal experiment regulations and the Swiss Federal Veterinary Office guidelines. Six- to 10-wk-old C57BL/6J and BALB/c mice were purchased from The Jackson Laboratory.

**Reagents.** Nano-sized particles ($TiO_2$, anatase, 20 nm; $TiO_2$, rutile, 80 nm; ZnO, 15 nm; $SiO_2$, 15 nm, carbon nanotubes) were obtained from Iolitec. Before each use, the particles were sonicated 15 min and vigorously vortexed for 1 min. Nigericin, MSU, cytochalasin D, nystatin, methyl-β-cyclodextrin, and chlorpromazine hydrochloride were purchased from Sigma; phorbol 12-myristate 13-acetate and APDC from Alexis.

Anti-human cleaved IL-1β (2021L) was purchased from Cell Signaling and anti-human caspase-1 (sc-622) was obtained from Santa Cruz; anti-IL-1β p35 is a sheep antibody made in our laboratory. Antibodies against mouse IL-1β and mouse caspase-1 (p20) were generous gifts from Roberto Solari, Glaxo, and Peter Vandenabeele (Ghent University, Belgium).

For cytokine detection, ELISA kits for murine IL-1α (R&D System), IL-1β, and TNF-α (eBioscience) were used according to the manufacturers' instructions.

**Cell Preparation.** Bone marrow-derived dendritic cells and bone marrow-derived macrophages were differentiated from tibial and femoral bone marrow progenitors as described elsewhere (29, 30). Cells were primed with 10 ng/mL ultra-pureLPS (Invivogen) for 3 h. Cell culture medium was replaced by OPTIMEM (Invitrogen) for the duration of the stimulation. Supernatants (SN) were precipitated by methanol-chloroform precipitation and cell extracts (XT) and SN of ≈200,000 cells were loaded for Western blot.

Primary adult murine tail epidermal keratinocytes were isolated from adult mice according to standard procedure (31). Tail skin was digested overnight in

10 mg/mL Dispase II (Roche). After removal of the epidermal sheets and trypsin digestion (0.05% Trypsin/EDTA), the epidermal suspension was filtered through a 100-μm mesh. The cells were cultured in Cnt-57 basal keratinocytes medium (CellnTec) on collagen-coated dishes (Purecol, Nutacon).

Primary human keratinocytes were isolated from neonatal foreskin (32). Briefly, the s.c. fatty tissue was trimmed and the biopsies were placed in 10 mg/mL Dispase II (Roche). The epidermal sheets were removed, chopped, and incubated in 0.05% Trypsin/EDTA. After filtration through a 100-μm mesh, the cells were cultured in Cnt-57 basal keratinocytes medium (CellnTec).

**Generation of THP1 Cells Stably Expressing shRNA.** THP1 cells stably expressing shRNA against Nalp3 and Caspase-1 were obtained as previously described (13).

For experiments, THP1 cells were differentiated 3 h with 0.5 μM phorbol 12-myristate 13-acetate (Enzo Lifesciences). Cell extracts and precipitated supernatants were analyzed by Western blot.

**Electron Microscopy.** Samples were fixed in 2% paraformaldehyde, 2.5% glutaraldehyde, and postfixed in 1% osmium tetroxide, 1.5% potassium ferrocyanide, and stained with 1% uranyl acetate. After dehydration, the samples were embedded in Durcupan. Ultrathin sections were contrasted with lead citrate and then examined with a Philips CM12 electron microscope.

**Fluorescence Microscopy.** Cholera toxin B staining (Invitrogen) was performed according to the manufacturer´s instructions. Slides were examined with a Leica SP5 tandem upright confocal microscope and the LAS AF lite software.

**In Vivo Peritonitis Model.** Peritonitis was induced in 6- to 10-wk-old age- and sex-matched mice by injection of 1–1.5 mg of sonicated and thoroughly vortexed $TiO_2$ particles in 400 μL sterile PBS. After 5–6 h, the mice were killed by $CO_2$ exposure and the peritoneal cavity was flushed with 5.5 mL of sterile PBS. The lavage fluid was centrifuged and the cell pellets analyzed for neutrophil influx by flow cytometry ($CD11b^+$, Ly-$6C^+$, Ly-$6G^{high}$, F4/$80^-$) using the following monoclonal antibodies: anti-CD11b (M1/70), anti-F4/80 (BM8) (eBioscience), anti–Ly-6C (AL-21), and anti–Ly-6G (1A8) (BD Biosciences). Data were collected using a FACSCanto (BD Biosciences) and analyzed using FLOWJO software (Tree Star).

The supernatants were concentrated using Amicon Ultra centrifugal filters (Millipore) and analyzed using ELISA kits for murine IL-1α (R&D System), IL-1β, IL-6, and TNF (eBioscience) according to the manufacturers' instructions.

For experiments in which IL-1α was blocked with a neutralizing antibody, mice were injected with anti-IL–1α (clone ALF-161, eBioscience) 80 μg i.p., 30 min before $TiO_2$ stimulation.

**In Vivo Cutaneous Exposure.** Intact murine back skin was challenged with nano-$TiO_2$ in PBS/olive oil or the PBS/olive oil carrier control by cutaneous exposure on the back skin. The back skin of the mice was shaved 24 h before exposure. Besides a single application, we applied the topical treatment daily for 5–10 consecutive days. Twenty-four hours after the last exposure, mice were killed by $CO_2$ exposure, skin biopsies were taken, fixed in formalin, and stained with hematoxylin and eosin (H&E) using standard procedures.

**In Vivo Intranasal Application and Bronchoalveolar Lavage (BAL).** $TiO_2$ (7.5–30 mg/kg) in saline or the vehicle alone was administered by nasal instillation in a volume of 40 μL under light ketamine-xylasine anesthesia. Six hours post-application, BAL was performed. Briefly, the trachea was incised and a homemade small plastic canula was inserted to flush both lungs three times with 1 mL PBS, going back and forth twice each time. The recovery of the total lavage exceeded 95%. The samples collected were centrifuged (600 *g* for 10 min) and cell pellets were resuspended in 0.4 mL PBS and maintained at 4 °C until cell determination. Differential cell counts were performed on cytospin preparations (Cytospin 3, Thermo Shandon) after May–Grünwald staining (Sigma) according to the manufacturer´s instructions. Differential cell counts were made on 200 cells using standard morphological criteria. For cytokine determination, the supernatants of the BALF were analyzed by ELISA.

After BAL, the lungs were perfused with Isoton (Coulder) to flush the vascular content. Lungs were homogenized by a rotor-stator (Ultra Turrax), the extract was centrifuged, and IL-1α and IL-1β levels in the supernatants of the lung homogenates were determined using ELISA.

**Statistical Analysis.** The significance of the differences between groups was calculated using the unpaired *t* test and the Bonferroni posttest (GraphPad Prism version 5.0). Differences were considered significant when $P < 0.05$.

**ACKNOWLEDGMENTS.** We thank Rosa Castillo for excellent technical support, Graham W. Knott for precious help with the electron microscopy, Mark Masin for establishing the cholera toxin staining, and Kate Schroder for helpful discussions and the critical reading of the manuscript. A.S.Y. is supported by Grant YA-182/1-1, Deutsche Forschungsgemeinschaft.

1. Auffan M, et al. (2009) Towards a definition of inorganic nanoparticles from an environmental, health and safety perspective. *Nat Nanotechnol* 4:634–641.
2. Klein J (2007) Probing the interactions of proteins and nanoparticles. *Proc Natl Acad Sci USA* 104:2029–2030.
3. Onuma K, et al. (2009) Nano-scaled particles of titanium dioxide convert benign mouse fibrosarcoma cells into aggressive tumor cells. *Am J Pathol* 175:2171–2183.
4. ILSI Risk Science Institute Workshop Participants (2000) The relevance of the rat lung response to particle overload for human risk assessment: A workshop consensus report. *Inhal Toxicol* 12:1–17.
5. Garabrant DH, Fine LJ, Oliver C, Bernstein L, Peters JM (1987) Abnormalities of pulmonary function and pleural disease among titanium metal production workers. *Scand J Work Environ Health* 13:47–51.
6. Bermudez E, et al. (2002) Long-term pulmonary responses of three laboratory rodent species to subchronic inhalation of pigmentary titanium dioxide particles. *Toxicol Sci* 70:86–97.
7. Inoue K, et al. (2008) Size effects of nanomaterials on lung inflammation and coagulatory disturbance. *Int J Immunopathol Pharmacol* 21:197–206.
8. Ferin J, Oberdörster G, Penney DP (1992) Pulmonary retention of ultrafine and fine particles in rats. *Am J Respir Cell Mol Biol* 6:535–542.
9. Sager TM, Kommineni C, Castranova V (2008) Pulmonary response to intratracheal instillation of ultrafine versus fine titanium dioxide: Role of particle surface area. *Part Fibre Toxicol* 5:17.
10. Kavita U, Mizel SB (1995) Differential sensitivity of interleukin-1 alpha and -beta precursor proteins to cleavage by calpain, a calcium-dependent protease. *J Biol Chem* 270:27758–27765.
11. Chen CJ, et al. (2007) Identification of a key pathway required for the sterile inflammatory response triggered by dying cells. *Nat Med* 13:851–856.
12. Martinon F, Burns K, Tschopp J (2002) The inflammasome: A molecular platform triggering activation of inflammatory caspases and processing of proIL-beta. *Mol Cell* 10:417–426.
13. Pétrilli V, et al. (2007) Activation of the NALP3 inflammasome is triggered by low intracellular potassium concentration. *Cell Death Differ* 14:1583–1589.
14. Gross O, et al. (2009) Syk kinase signalling couples to the Nlrp3 inflammasome for anti-fungal host defence. *Nature* 459:433–436.
15. Willingham SB, et al. (2009) NLRP3 (NALP3, Cryopyrin) facilitates in vivo caspase-1 activation, necrosis, and HMGB1 release via inflammasome-dependent and -independent pathways. *J Immunol* 183:2008–2015.
16. Mariathasan S, et al. (2006) Cryopyrin activates the inflammasome in response to toxins and ATP. *Nature* 440:228–232.
17. Martinon F, Pétrilli V, Mayor A, Tardivel A, Tschopp J (2006) Gout-associated uric acid crystals activate the NALP3 inflammasome. *Nature* 440:237–241.
18. Feldmeyer L, et al. (2007) The inflammasome mediates UVB-induced activation and secretion of interleukin-1beta by keratinocytes. *Curr Biol* 17:1140–1145.
19. Hornung V, et al. (2008) Silica crystals and aluminum salts activate the NALP3 inflammasome through phagosomal destabilization. *Nat Immunol* 9:847–856.
20. Dostert C, et al. (2008) Innate immune activation through Nalp3 inflammasome sensing of asbestos and silica. *Science* 320:674–677.
21. Schroder K, Tschopp J (2010) The inflammasomes. *Cell* 140:821–832.
22. Sadrieh N, et al. (2010) Lack of significant dermal penetration of titanium dioxide from sunscreen formulations containing nano- and submicron-size TiO2 particles. *Toxicol Sci* 115:156–166.
23. Filipe P, et al. (2009) Stratum corneum is an effective barrier to TiO2 and ZnO nanoparticle percutaneous absorption. *Skin Pharmacol Physiol* 22:266–275.
24. Johnston HJ, et al. (2009) Identification of the mechanisms that drive the toxicity of TiO(2) particulates: The contribution of physicochemical characteristics. *Part Fibre Toxicol* 6:33.
25. Kuida K, et al. (1995) Altered cytokine export and apoptosis in mice deficient in interleukin-1 beta converting enzyme. *Science* 267:2000–2003.
26. Mariathasan S, et al. (2004) Differential activation of the inflammasome by caspase-1 adaptors ASC and Ipaf. *Nature* 430:213–218.
27. Horai R, et al. (1998) Production of mice deficient in genes for interleukin (IL)-1alpha, IL-1beta, IL-1alpha/beta, and IL-1 receptor antagonist shows that IL-1beta is crucial in turpentine-induced fever development and glucocorticoid secretion. *J Exp Med* 187:1463–1475.
28. Adachi O, et al. (1998) Targeted disruption of the MyD88 gene results in loss of IL-1- and IL-18-mediated function. *Immunity* 9:143–150.
29. Gross O, et al. (2006) Card9 controls a non-TLR signalling pathway for innate anti-fungal immunity. *Nature* 442:651–656.
30. Didierlaurent A, et al. (2006) Tollip regulates proinflammatory responses to interleukin-1 and lipopolysaccharide. *Mol Cell Biol* 26:735–742.
31. Redvers RP, Li A, Kaur P (2006) Side population in adult murine epidermis exhibits phenotypic and functional characteristics of keratinocyte stem cells. *Proc Natl Acad Sci USA* 103:13168–13173.
32. Calkins CC, et al. (2006) Desmoglein endocytosis and desmosome disassembly are coordinated responses to pemphigus autoantibodies. *J Biol Chem* 281:7623–7634.